Flow rates and crystal orientation fabrics in compression of polycrystalline ice at low temperatures and stresses

Tim H. Jacka and Li Jun

Antarctic CRC and Australian Antarctic Division, Box 252-80, Hobart, Tasmania 7001, AUSTRALIA

Abstract: Results of laboratory deformation tests are presented for uniaxial compression creep on isotropic ice samples over the temperature range –10 to –45 °C and stress range 0.8 to 0.1 MPa. We examine the effect of reducing temperature and stress on the development of anisotropic crystal structure, and the magnitude of the steady state tertiary strain rate in this stress configuration relative to the isotropic minimum strain rate (i.e. the enhancement factor). We find that for lower temperatures and stresses, the enhancement factor decreases to a value of 1 (no enhancement) as the crystal fabric strength reduces from a strong small circle girdle pattern at higher temperatures and stresses, to approximately random at lower temperatures and stresses.

The results support the conclusion that at higher temperatures and stresses, the dominant deformation mechanism is recrystallization, while at lower temperatures and stresses crystal rotation may be more important.

Introduction

For polycrystalline initially isotropic ice in unconfined uniaxial compression to strain, ε, the creep curve exhibits a primary stage ($\ddot{\varepsilon} < 0$), a minimum (still isotropic, secondary) strain rate ($\dot{\varepsilon} = \dot{\varepsilon}_{min}$, $\ddot{\varepsilon} = 0$), an accelerating (recrystallization) stage ($\ddot{\varepsilon} > 0$) and finally a steady sate (anisotropic, tertiary) strain rate ($\dot{\varepsilon} = \dot{\varepsilon}_{ss}$, $\ddot{\varepsilon} = 0$) as shown in Fig. 1[1]. An enhancement factor, E for the anisotropic steady state strain rate relative to the minimum isotropic strain rate can be defined as

$$E = \dot{\varepsilon}_{ss} / \dot{\varepsilon}_{min} .$$

For unconfined uniaxial compression laboratory experiments, E has consistently been found to have a value of 3.

The crystal orientation fabric pattern resulting from this deformation has consistently been found (for cylindrical samples in which the radial strain is equal in all directions) to be a small circle girdle with half cone angle ~ 25 to 30° [1, 2]. Small circle girdle crystal orientation fabrics are also exhibited in several of the ice cores extracted from the natural ice masses. Fig. 2 shows some examples from locations in Antarctica and Greenland (detailed in Table 1) of crystal orientation fabrics that indicate a trend towards the development of a small circle girdle pattern.

Physics of Ice Core Records
Edited by T. Hondoh
Hokkaido University Press, 2000, Sapporo

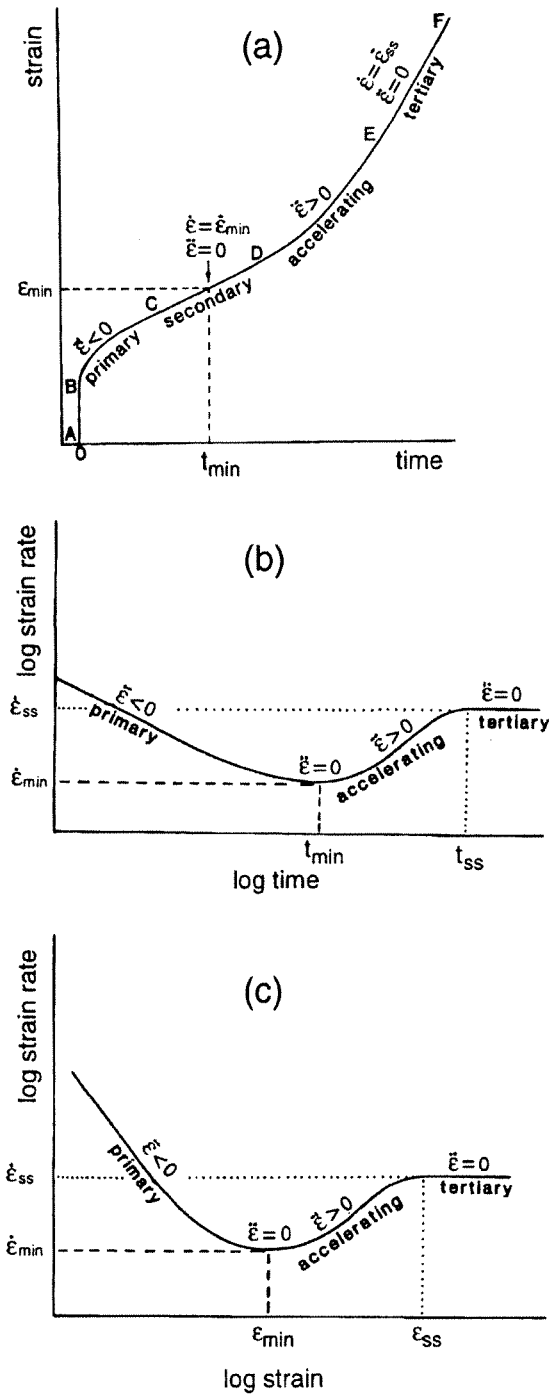

Figure 1: (a) An idealized creep curve for ice shows the various stages of strain, ε versus time, t as follows: A–B: the initial impulsive elastic strain, B–C, C–D, D–E, and E–F the primary, secondary, accelerating and tertiary stages. (b) The corresponding log strain rate versus log time plot is shown indicating the minimum and "steady state" tertiary strain rates. (c) The corresponding log strain rate versus log strain plot shows the same features (after Budd and Jacka [1]).

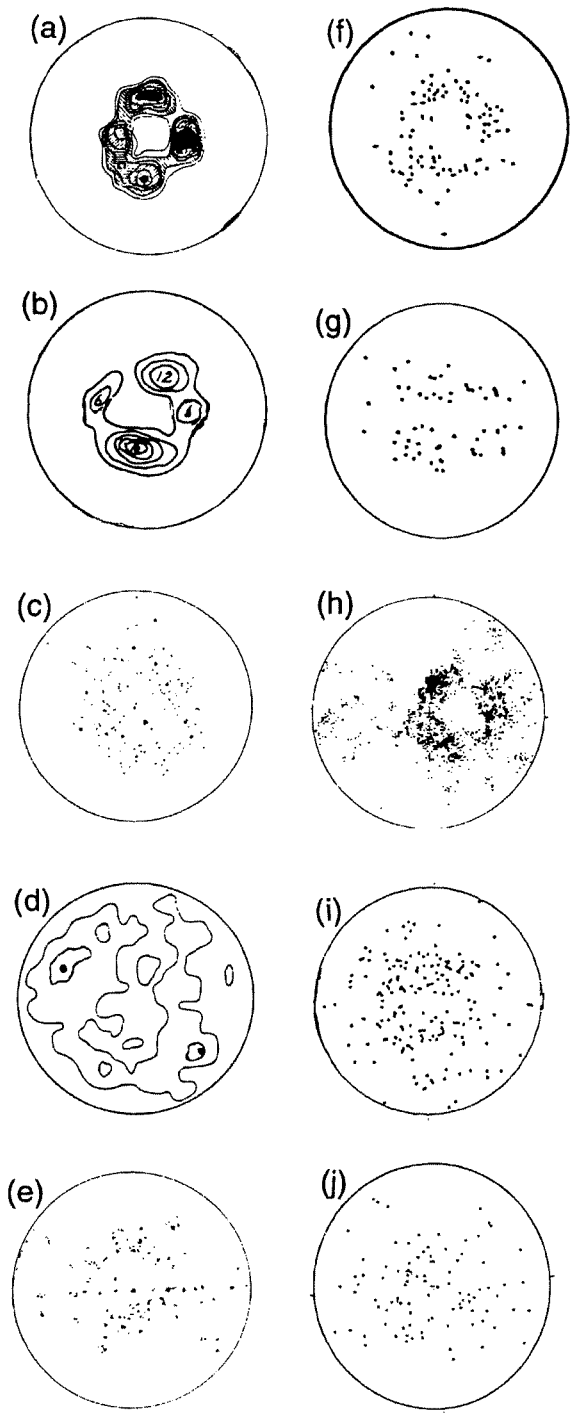

Figure 2: Selected crystal orientation fabrics measured in ice cores drilled at various locations in Antarctica and Greenland, each exhibiting the development of a small circle girdle orientation pattern.

Table 1: Details of crystal orientation fabric patterns shown in Fig. 2.

Fig. 2	Location	Depth (m)	Reference
(a)	Ross Ice Shelf, Antarctica	249	3)
(b)	Amery Ice Self, Antarctica	155	4)
(c)	Byrd Station, W. Antarctica	439	5)
(d)	Camp Century, Greenland	229	6)
(e)	Dye 3, Greenland	695	7)
(f)	Law Dome summit (A001)	318	8)
(g)	Law Dome (BHQ)	160	9)
(h)	Law Dome - Cape Folger	*	10)
(i)	GRIP, Greenland	689	11)
(j)	GISP2, Greenland	601	12)

** this fabric consists of an accumulation of data from several depths.*

In Fig. 3, the laboratory development of the small circle girdle crystal fabric pattern is compared with the change in fabric pattern with depth through an ice core drilled at the summit of Law Dome, East Antarctica, culminating in the final fabric, (f) of Fig. 2, at a depth of 318 m.

The laboratory results have emanated from experiments in the temperature range −0.01 [13] to −10.0 °C and stress range 0.1 to 1.0 MPa, such that minimum and tertiary steady state strain rates were attainable in a manageable (typically less than 1 year) time period. Note also that the ice cores in which the clearest developments of the small circle girdle fabric have been found have generally been from areas of relatively high snow accumulation rate (e.g. ice shelves, the summit area of Law Dome). High accumulation rate leads to increased values of strain rate at relatively shallow depths in the polar ice masses, and thus to accelerated fabric development. Incidentally, if the accumulation is high enough, this may also lead to a sharp increase in crystal growth rate at the firn/ice transition, where stress effects dominate over the temperature dependence of crystal growth [14].

It has been proposed from theoretical considerations of crystal rotation that in compression to high strains, a single maximum crystal orientation fabric pattern develops with symmetry axis parallel to the compression axis [15–19]. Fig. 4 shows the simulated development of the single maximum pattern under uniaxial compression from Azuma and Higashi [17]. These considerations have involved rotation only and neglected recrystallization, which it has been argued, is inhibited at low temperatures and stresses.

Assuming that both the laboratory results at higher temperatures and stresses, and the theoretical considerations at lower temperatures and stresses are correct, some interesting issues arise. First, the single pole fabric pattern is a "hard glide" pattern for uniaxial compression parallel to the

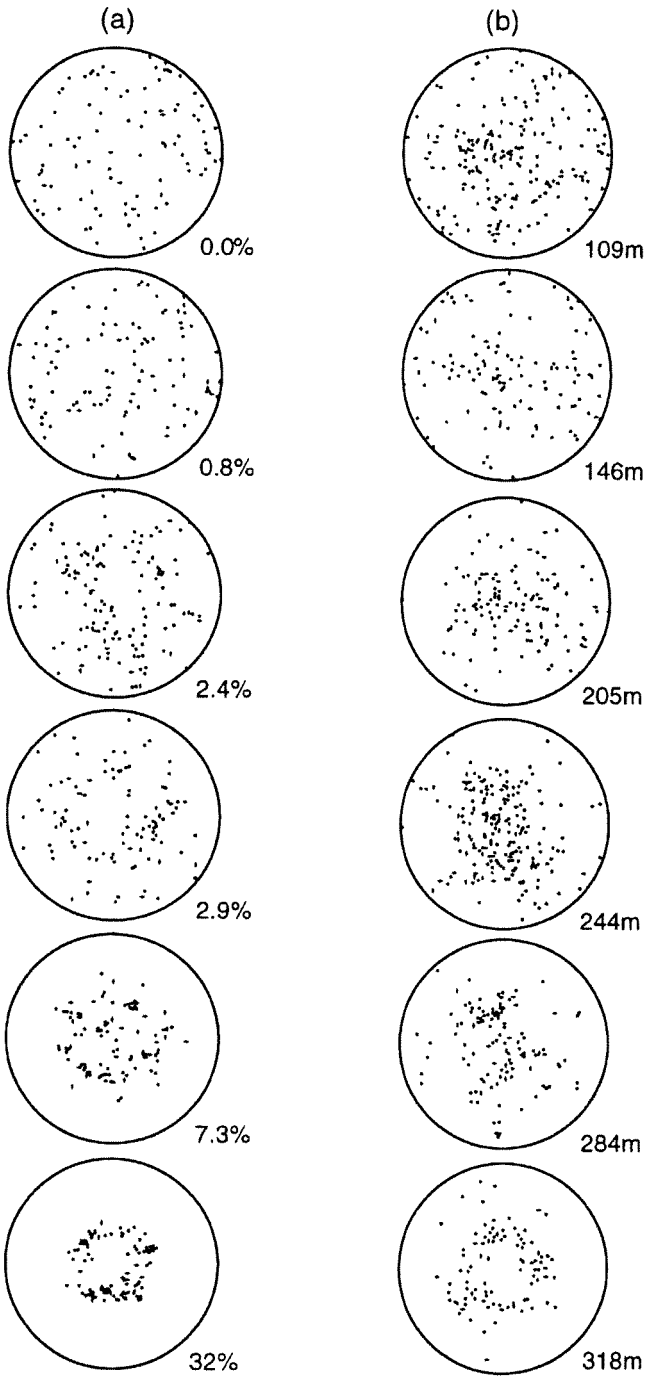

Figure 3: Measured crystal orientation fabrics from (a) laboratory experiments, beginning with a laboratory prepared isotropic sample, to various levels of uniaxial compressive strain (from Jacka and Maccagnan [2]), and (b) various depths from an ice core drilled at the summit (a near stationary point) of Law Dome, East Antarctica (from Gao and Jacka [8]).

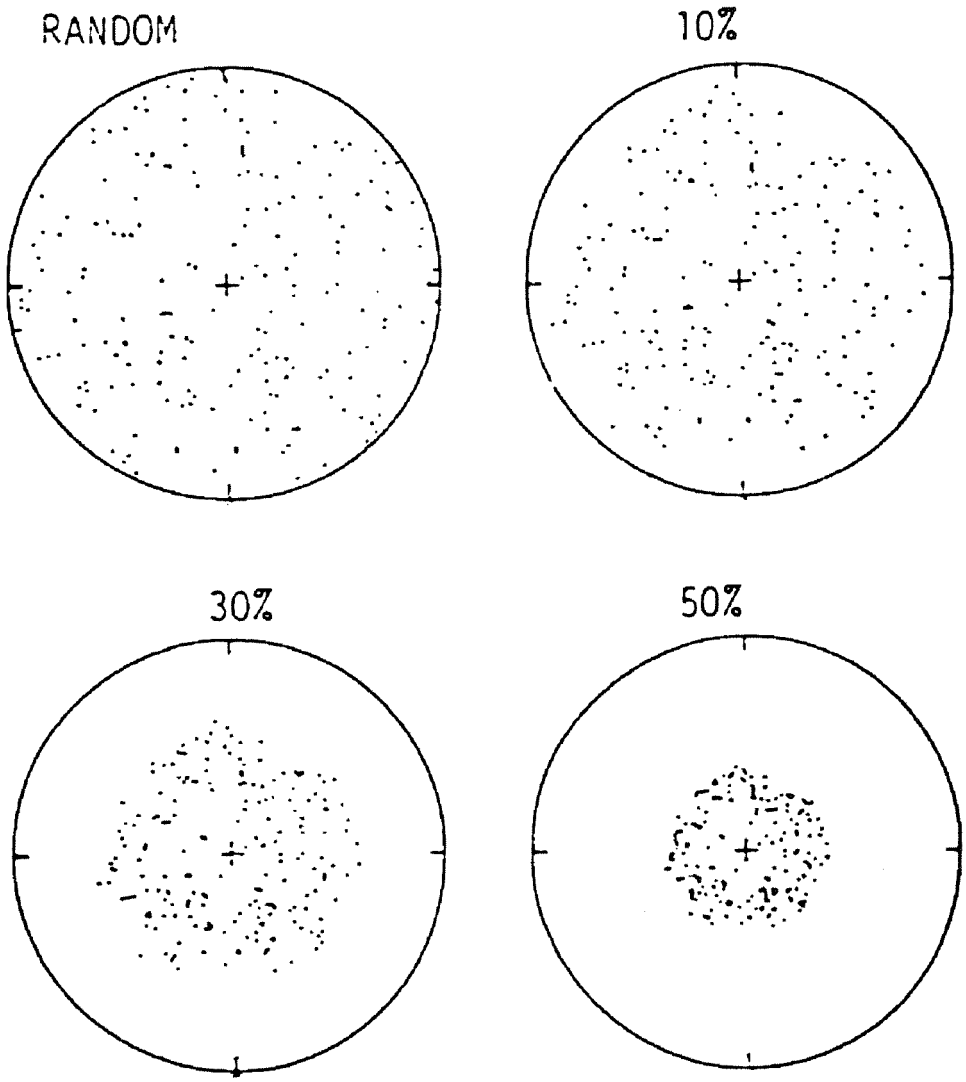

Figure 4: Simulated crystal orientation fabrics, beginning with a random fabric, after various levels of uniaxial compressive strain. The simulation assumes rotation but no recrystallization processes during the deformation (after Azuma and Higashi [17]).

symmetry axis of the pole. Fig. 5 from Jacka and Budd [20] demonstrates this. The minimum strain rate in compression for the sample exhibiting a single maximum fabric is lower, not only than the minimum strain rate for the sample with small circle fabric, but even than the minimum strain rate for the sample with random crystal structure. That is, the flow rate for this deformation/crystal orientation configuration is lower, even than the minimum flow rate of isotropic ice. Thus the case for single pole development implies a configuration in which the crystals rotate

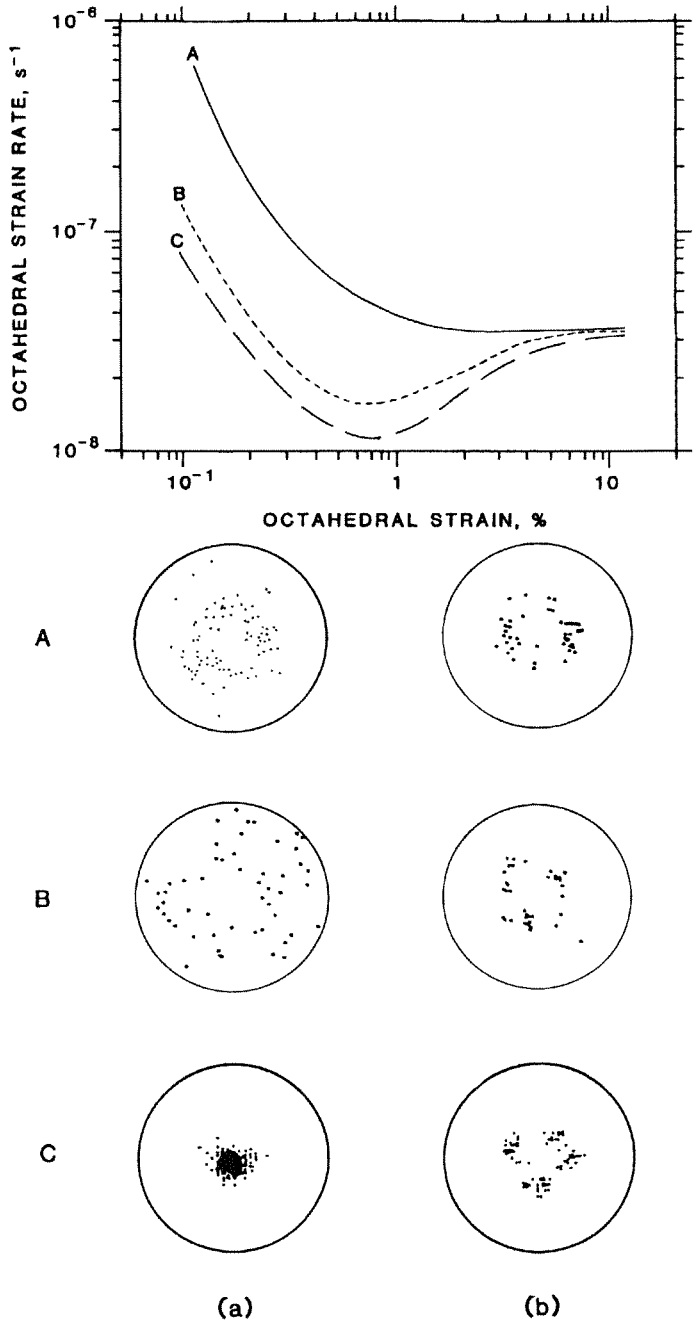

Figure 5: Creep curves for three deformation tests in uniaxial compression at –3.3 °C and 0.2 MPa. Curve A: initially anisotropic ice exhibiting a small circle girdle orientation fabric; Curve B: initially isotropic ice; and Curve C: initially anisotropic ice exhibiting a single maximum fabric pattern. Curve A illustrates easy glide in compression; Curve C illustrates hard glide (at the minimum strain rate) in compression. Crystal orientation fabrics exhibited (a) prior to testing and (b) at test completion are also shown. Note that in all cases the final (steady state) crystal fabric pattern (at this stress and temperature) was a small circle girdle (after Jacka and Budd [20]).

away from the direction most favourable for deformation. This certainly would imply that the use of the term "preferred crystal orientation fabric" (which would seem to imply increasing strain rates) should be ceased.

Second, given steady state (anisotropic) strain rates higher than the isotropic minimum strain rate (by a factor of 3) for higher temperatures and stresses, and lower strain rates at lower temperatures and stresses, what is the nature of the transition from higher to lower strain rates, i.e. from the creep of ice predominantly undergoing migration recrystallization to that predominantly undergoing rotation recrystallization? It seems logical that there should be some region where (with decreasing temperature and stress) rotation recrystallization takes over from migration recrystallization as the dominant mechanism. We might for example, expect "easy glide" ($E > 1$) for the higher temperatures and stresses, "hard glide" ($E < 1$) for the lower temperatures and stresses and an intermediate or balance condition ($E = 1$) at some (or a range of) intermediate temperature and stress. Assuming the flow of isotropic ice is governed by a law of the form [21] $\dot{\varepsilon}_o = E\ A\ \tau_o^n$ ($E = 1$; A is a temperature dependent constant; τ is the stress deviator tensor; subscript "o" denotes octahedral or root mean square values, in which case laboratory evidence [22] demonstrates that isotropic flow rates are independent of stress pattern) with n constant, the above description leads to an anisotropic flow law for compression that may be similar to the sketch of Fig. 6. Note also that the steady state crystal orientation fabric pattern for simple shear is a single maximum pattern over the full range of temperatures and pressures, at least existing in the natural ice masses on Earth. This is because recrystallization and rotation processes both lead to the development of this fabric. Furthermore we know from laboratory and field experiments that the flow rate of ice exhibiting this fabric in simple shear is a factor of about 10 greater [22] than the flow of isotropic ice.

Given that we have an intermediate region with $E = 1$, what is the nature of the crystal orientation fabric pattern in this region? Does it remain random indefinitely - this would facilitate values of $E = 1$ (tertiary strain rates unchanged from those at minimum isotropic strain rate). Or, does it change to some other pattern intermediate between a small circle girdle and a single pole pattern? Can we find these crystal patterns in the polar ice cores?

In order to address these issues, we have carried out a suite of uniaxial compression tests aimed at attaining minimum and tertiary creep at low temperatures (as low as –45 °C) and stresses (as low as 0.1 MPa). Some of these tests have been running (at time of publication) for 5 years.

Test conditions

The creep deformation apparatus used for the compression tests is the direct load (constant stress) apparatus described by Jacka and Lile [23]. We have several of these apparatus, which are operated in freezer boxes (one of which is capable of maintaining temperatures as low as –60 °C) set at temperatures below the test temperature. Accurate experiment temperature control is maintained by heating a silicone oil bath surrounding the ice test sample [24]. Digital displacement dial

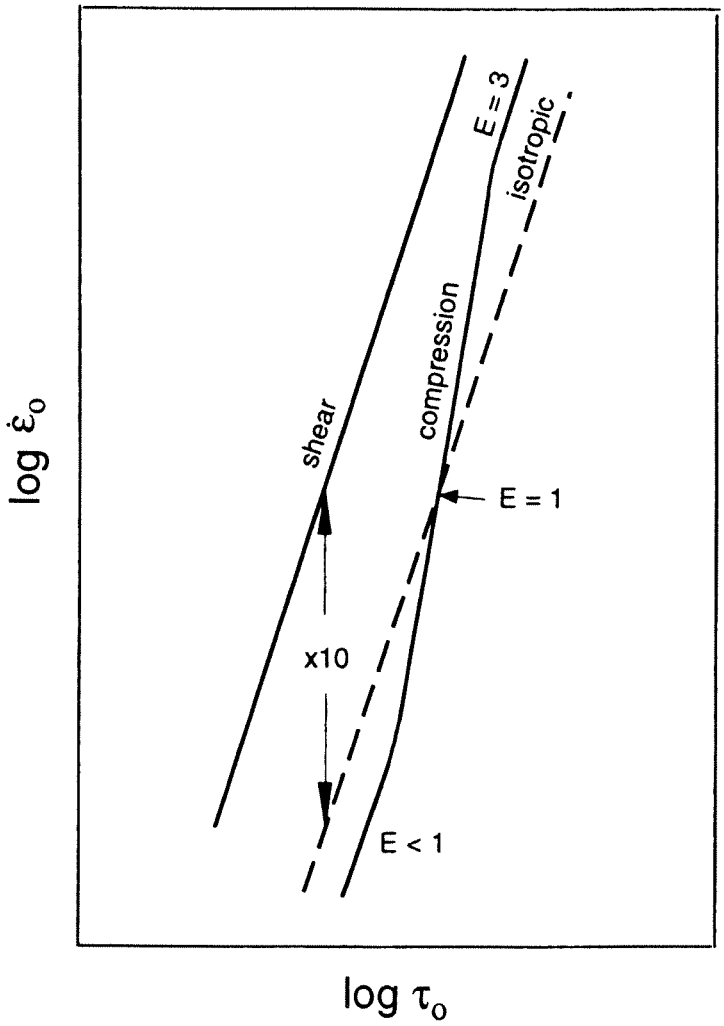

Figure 6: Sketch illustrating possible relationship between octahedral strain rate, $\dot{\varepsilon}_o$ and octahedral stress, τ_o for steady state anisotropic ice flow (solid lines), relative to an assumed isotropic ice flow power law (dashed line). For anisotropic shear flow, an enhancement over isotropic flow rate, $E = 10$ is assumed. For compression, $E = 3$ is assumed at high stresses, $E < 1$ is assumed for low stresses and $E = 1$ is assumed at some intermediate stress.

indicators monitor the ice sample strain, directly to a PC on which analysis for strain rate is carried out. We can remove a tested sample from the apparatus, cut it for thin section analysis, machine it back to its original shape then re-load and re-test the sample.

The ice test samples were laboratory prepared initially cylindrical (60 mm long; 25.4 mm diameter), with randomly oriented, small grained crystal structure [23].

Results

Table 2 shows the range of temperatures and stresses examined. There are sufficient tests to independently

Table 2: Stress (MPa) and temperature (°C) range of experiments covered by the study.

Stress MPa \ Temperature °C	-5	-10	-15	-19	-21	-45
0.8				•		
0.55					•	• •
0.5			•			
0.4			•	•		
0.3			•	•		
0.2	•	•	•	•	•	
0.1			•	•		

examine effects of reducing stress with temperature fixed, and reducing temperature with stress fixed. In addition, an additional test at –45 °C provides further information at lower temperatures. For each test, we present a creep curve, i.e. a plot of octahedral (root mean square of the principal deviator tensor) strain rate as a function of octahedral strain. We have "normalized" the strain rates so that the strain rate at a strain of 1 % is assigned a value of 1. Actual measured strain rate values along with enhancement factors are listed in Table 3. Previous laboratory studies [1] have shown that the minimum isotropic strain rate generally occurs at about 1 % octahedral strain. This normalization allows us to easily examine the flow rates in terms of E. The dashed horizontal lines across each plot indicate values of 1 - the isotropic strain rate at 1 % strain, and 3 - the (relative) steady state anisotropic strain rate at the higher stresses and temperatures, i.e. for the case in which migration recrystallization is dominant.

Along with most creep curves, we present a Schmidt equal area c-axis fabric diagram and a histogram of the frequency of crystals within each 5° c-axis inclination interval. These diagrams indicate the crystal structure at the test conclusion, recalling that the initial crystal pattern for each test

Table 3: Summary of test temperature, θ, octahedral stress, τ_o, minimum, $\dot{\varepsilon}_{min}$ and tertiary steady state $\dot{\varepsilon}_{ss}$, octahedral strain rates and enhancement factor, E, for tests described.

θ, °C	τ_O, MPa	$\dot{\varepsilon}_{min}$, s^{-1}	$\dot{\varepsilon}_{ss}$, s^{-1}	E
-45	0.55	4.2×10^{-10}		
-21	0.55	1.1×10^{-8}	2.3×10^{-8}	2.1
-21	0.2	8.0×10^{-10}	7.2×10^{-10}	0.9
-19	0.8	7.8×10^{-8}	2.1×10^{-7}	2.7
-19	0.4	8.9×10^{-9}	1.8×10^{-8}	2.0
-19	0.3	4.0×10^{-9}	6.8×10^{-9}	1.7
-19	0.2	1.1×10^{-9}	1.3×10^{-9}	1.2
-19	0.1	4.9×10^{-10}	4.9×10^{-10}	1.0
-15	0.5	3.4×10^{-8}	7.5×10^{-8}	2.2
-15	0.4	1.4×10^{-8}	3.6×10^{-8}	2.6
-15	0.3	7.2×10^{-9}	1.4×10^{-8}	1.9
-15	0.2	3.0×10^{-9}	3.3×10^{-9}	1.1
-15	0.1	7.0×10^{-10}	7.0×10^{-10}	1.0
-10	0.2	4.1×10^{-9}	6.6×10^{-9}	1.6
-5	0.2	1.1×10^{-8}	3.4×10^{-8}	3.1

was approximately random. The sine curve is the expected distribution for the case of randomly distributed c-axes. Thus for differences from isotropic, we need to consider the variation of the histograms from the sine curve.

Fixed temperature; decreasing stress

Fig. 7 shows the creep curves and fabric data for the series of tests at –15 °C and stress range 0.5 to 0.1 MPa. Fig. 8 shows the data for the tests at –19 °C over the stress range 0.8 to 0.1 MPa. Note to begin, that each curve follows the general

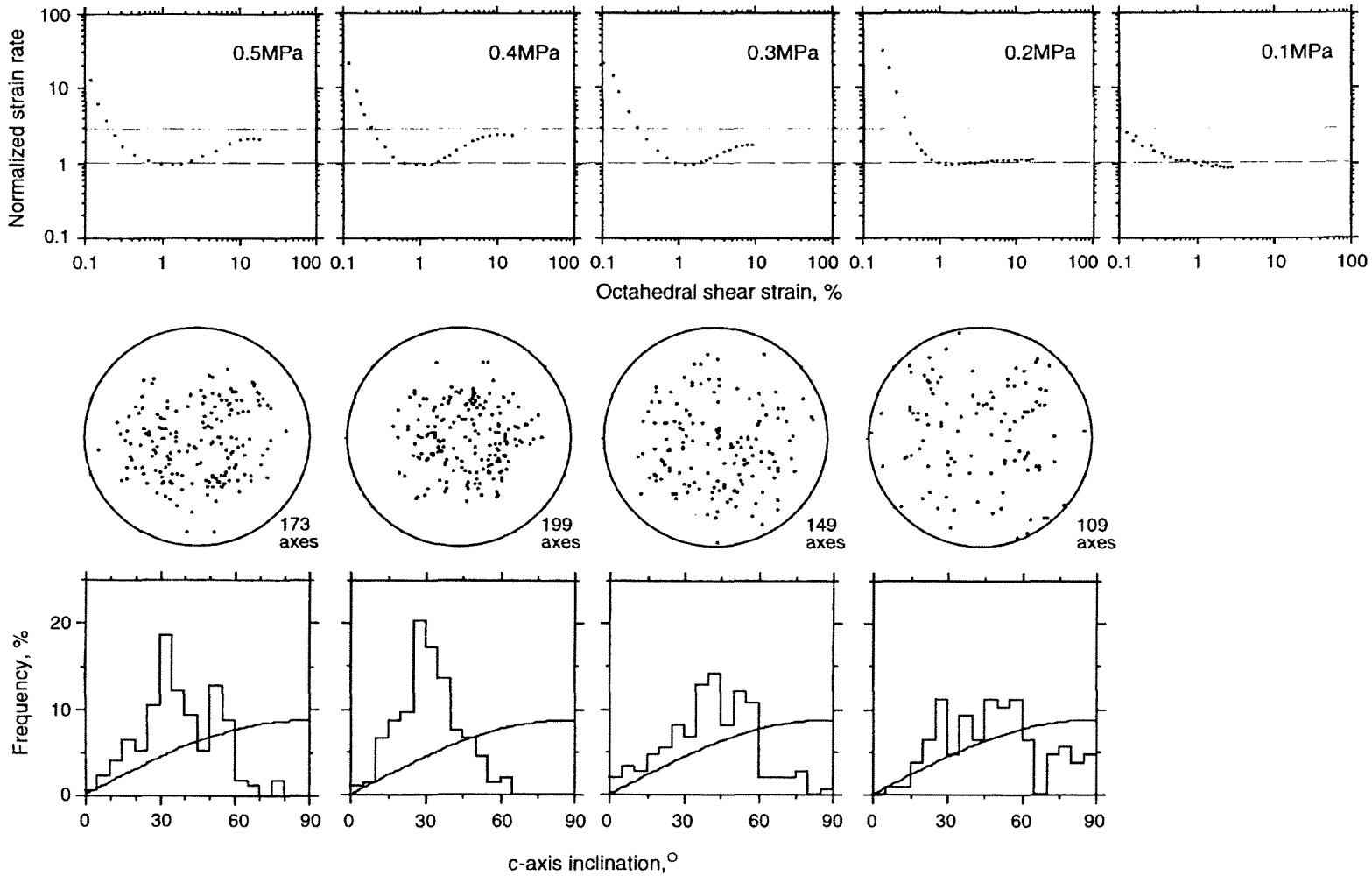

Figure 7: Creep curves (showing a "normalized" strain rate scale for comparison purposes) and fabric data for the series of tests at –15°C over the stress range 0.5 to 0.1 MPa.

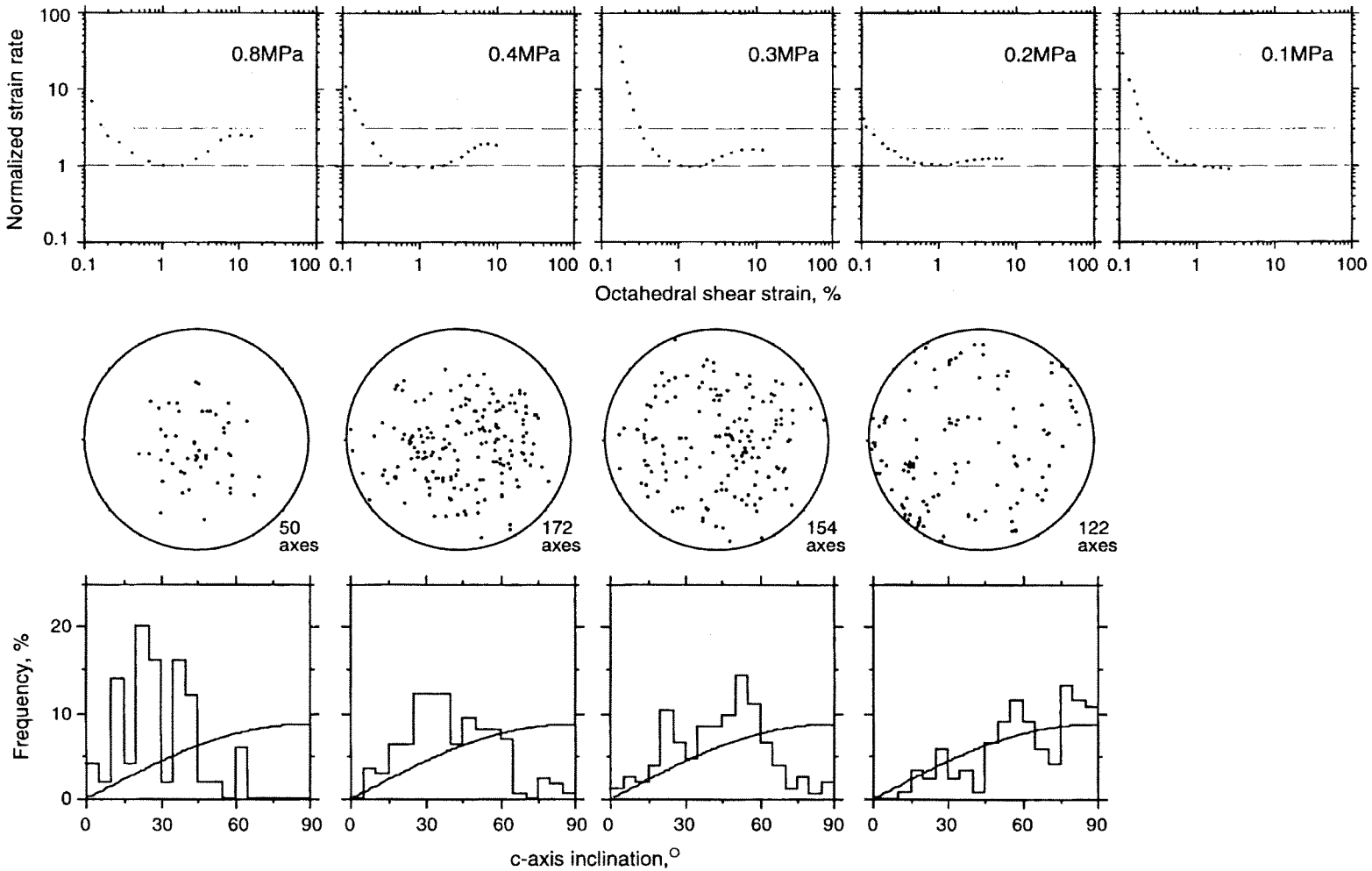

Figure 8: Creep curves (showing a "normalized" strain rate scale for comparison purposes) and fabric data for the series of tests at –19°C over the stress range 0.8 to 0.1 MPa.

shape described in the Introduction. For the test at −15 °C; 0.5 MPa, we see that the steady state creep rate is a factor of 2 to 3 greater than the minimum isotropic creep rate. The crystal fabric pattern at the test conclusion is a weak small circle girdle. Note in particular from the histogram, the concentration of c-axes occurring in the annulus 25 to 60° from the symmetry axis. The creep curve for −15 °C; 0.4 MPa shows a similar result, and the −19 °C; 0.8 MPa test also shows a similar result. Thus, at −15 °C; 0.5 and 0.4 MPa, and −19 °C; 0.8 MPa, the results are within the expectations of our past laboratory studies[1, 2].

The tests at −15 °C; 0.3 MPa and at −19 °C; 0.4 and 0.3 MPa exhibit tertiary strain rates greater than the minimum isotropic strain rate, but greater by a factor significantly less than 3, and reducing with reducing stress (note the −19 °C; 0.4 and 0.3 MPa tests particularly). The crystal fabrics at the conclusion of these 3 tests again indicate small circle patterns, but weakening with reducing stress (note the reducing amplitude, from left to right within the Figures, of the histogram peaks in the 25 to 60° range).

The 0.2 MPa tests at both −15 and −19 °C indicate tertiary strain rates only marginally greater than the minimum isotropic strain rate, despite strains of 7 % at −19 °C and 15 % at −15 °C. Recall that ~ 1 % strain was required to attain minimum strain rate for the tests at higher stresses. The crystal fabric pattern for the −15 °C; 0.2 MPa test is a very weak small circle, and the pattern for the −19 °C; 0.2 MPa test is not significantly different from random.

The −15 and −19 °C; 0.1 MPa tests appear to have attained minimum strain rates but as yet (the −15 °C test has reached 3 % strain and the −19 °C test has reached 2 %) there is no indication of an increase in strain rate. These two tests are continuing, thus there has so far been no crystal fabric analysis.

Summarizing the −15 and −19 °C tests in the range 0.8 to 0.1 MPa, there appears to be a consistent trend to decreasing tertiary strain rate enhancement over minimum isotropic strain rate (from 3 to 1) with decreasing stress. Along with this decrease, the strength of the small circle crystal orientation pattern decreases to the point where, for an enhancement factor of 1 (i.e. no enhancement), the pattern is not significantly different from random.

Fixed stress; decreasing temperature

Fig. 9 shows five tests (including two duplicated from Figs. 1 and 2) at a stress of 0.2 MPa, and temperatures of −5, −10, −15, −19 and −21 °C. For the −5 °C test, the tertiary strain rate is a factor of 3 greater than the isotropic minimum strain rate, and the resulting crystal orientation fabric is a strong small circle girdle. At −10 °C the tertiary strain rate is already less than a factor of 2 greater than the minimum isotropic strain rate. The crystal orientation fabric pattern is a weaker small circle pattern.

The −15 and −19 °C; 0.2 MPa results have been discussed above, showing tertiary strain rates only marginally greater than the minimum isotropic strain rate, along with fabric patterns of a very weak small circle for the −15 °C test and insignificantly different from random for the −19 °C test.

The −21 °C; 0.2 MPa test indicates a creep curve similar to the lower stress tests described above. The minimum strain rate,

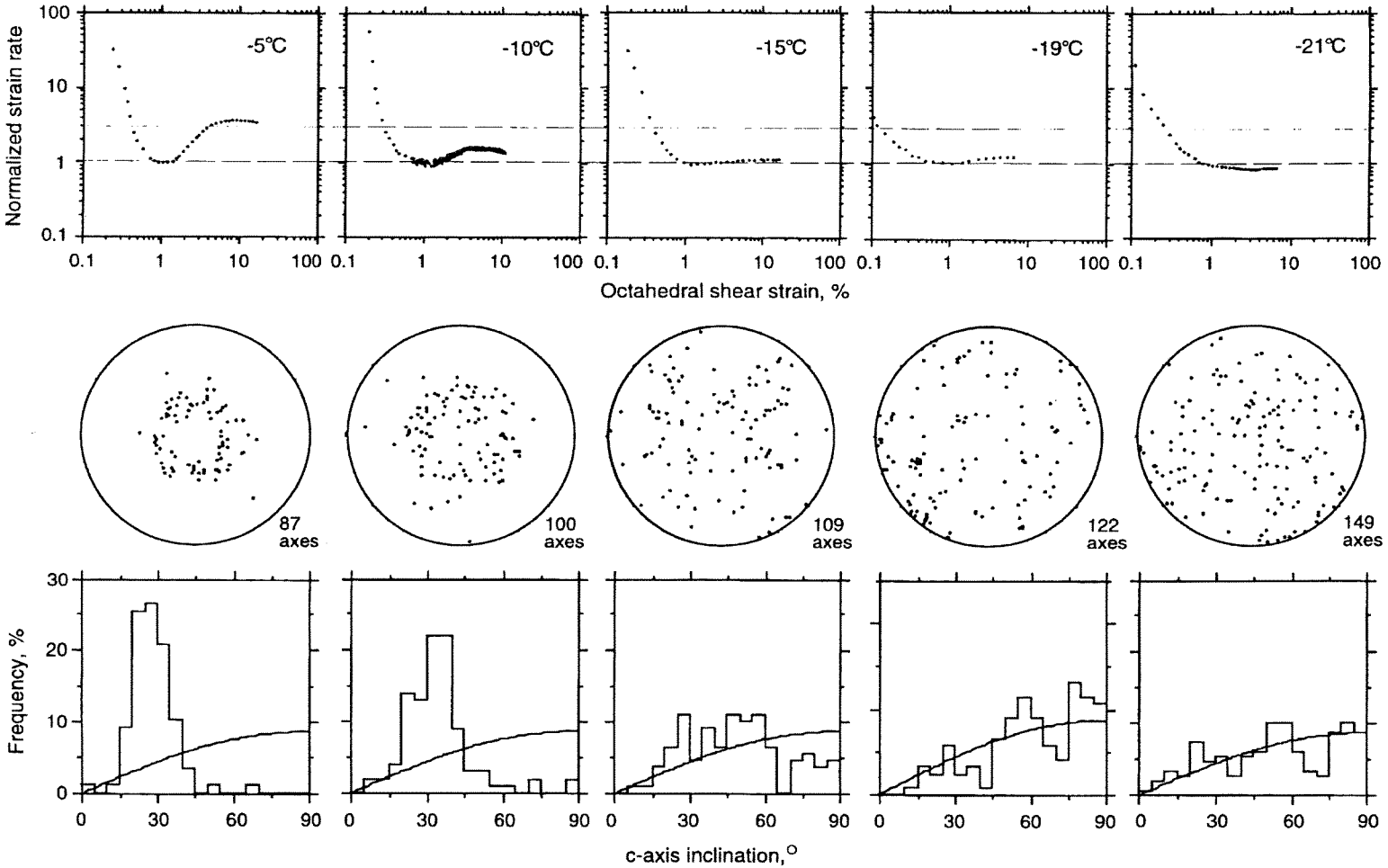

Figure 9: Creep curves (showing a "normalized" strain rate scale for comparison purposes) and fabric data for the series of tests at 0.2 MPa over the temperature range –5.0 to –21.0 °C.

attained (as expected) at ~ 1 % strain, is maintained over an extensive strain interval of ~ 7 %. The crystal orientation pattern at the conclusion of this test is not significantly different from random.

In summary, the pattern of change of the creep curves at a fixed stress of 0.2 MPa but over a reducing range of temperatures is similar to that obtained for a fixed temperature with reducing stress. That is, there is a consistent trend to decreasing tertiary strain rate enhancement with decreasing temperature, associated with decreasing small circle fabric strength until, with approximately random fabrics, there is no strain rate enhancement.

Further tests at lower temperatures

We examine two tests at a stress of 0.55 MPa and at temperatures of –21 and –45 °C. Fig. 10 shows results from these two tests. The –21 °C; 0.55 MPa test provides results similar to those described above. The tertiary strain rate is a factor of ~ 2 greater than the minimum isotropic strain rate, and the crystal fabric pattern at test conclusion is a very weak small circle girdle.

For the –45 °C; 0.55 MPa test we have indicated the actual strain rate values - we see why later. We stopped this test at ~ 3.5 % strain, in August 1997 (after 3 years testing) in order to present the creep curve and crystal fabric data to the European Ice Sheet Modelling Initiative (EISMINT) Ice Rheology Workshop in Grindelwald, Switzerland. The crystal fabric pattern was approximately random.

Another reason for stopping the test was a suspicion that there may have been displacement dial indicator sticking problems. On return to the laboratory from the EISMINT workshop, we machined the sample (which had been stored at –45 °C) back to its original geometry, re-loaded it into the deformation apparatus along with a new displacement dial indicator, and re-commenced the test. Since recovery of anelastic creep takes ~ 1 % strain [1], we expected it would be about 1 year before the strain rate stabilized at the value pertaining to the current crystal fabric pattern, and attained the same value it was at when we terminated the experiment.

The creep curve reported to the International Commission on Snow and Ice (ICSI) Workshop on "The Physics of Ice-Core Records" in Shikotsukohan, Japan in September 1998 (i.e. about one year after re-loading) exhibited a strain rate value of ~ 5×10^{-10} s^{-1} - as expected, the same as it had been a year earlier when the test was terminated. This would seem to validate the earlier result, and to render unlikely, any problem due to the displacement dial indicator sticking.

The creep curve at September 1999 (a further year later, and just prior to publication of this paper) is shown in Fig. 11. The strain rate has gone through a minimum (at ~ 4.2×10^{-10} s^{-1}) and is now increasing. Thus $E > 1$. However we do not yet have a final value for the enhancement factor. The experiment continues.

Discussion and conclusions

We are unable to confirm the development of a single pole fabric pattern (which would develop as a consequence of rotation recrystallization) at high strain in uniaxial compression. We are able to report that the enhancement of tertiary steady state

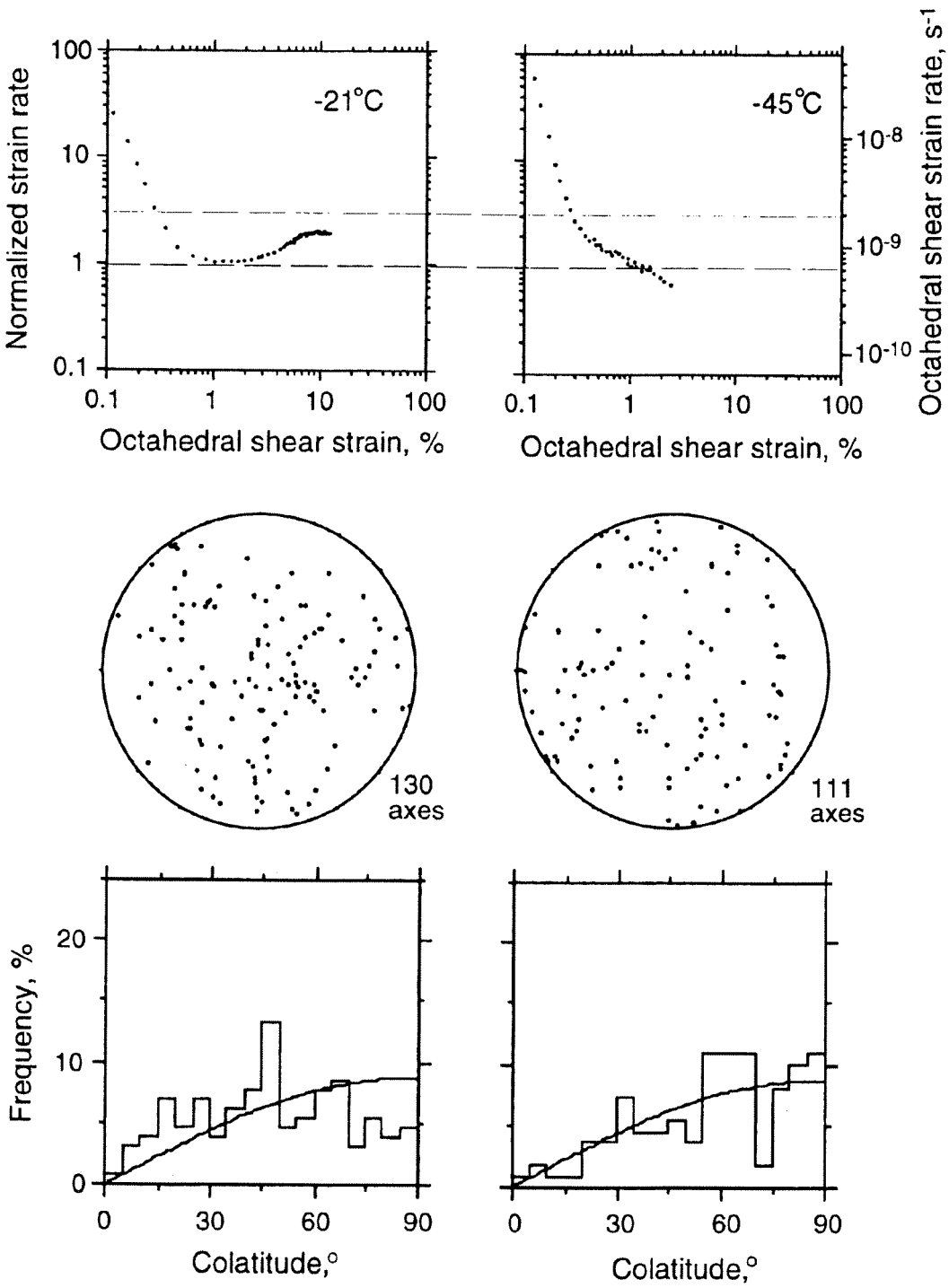

Figure 10: Creep curves and fabric data for tests at 0.55 MPa and temperatures of –21 and –45 °C. The strain rate scale on the right hand axis applies to the –45 °C test only, and is for comparison with Fig. 11.

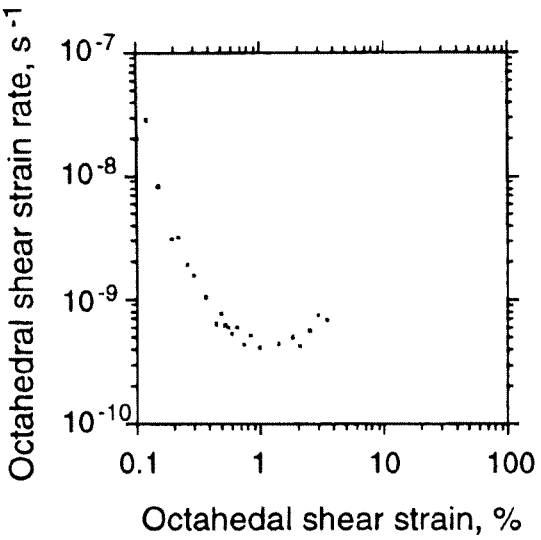

Figure 11: Creep curve for a re-test at 0.55 MPa and –45 °C on the same sample as shown in Fig. 10.

strain rate over minimum isotropic strain rate is reduced as a function of decreased temperature and as a function of decreased stress. In addition, the resulting crystal orientation fabric pattern, a small circle girdle at higher temperatures and stresses, seems to weaken with decreasing temperature and stress. This trend persists until strain rate enhancement is lost (E = 1) for a random fabric. We conclude from this

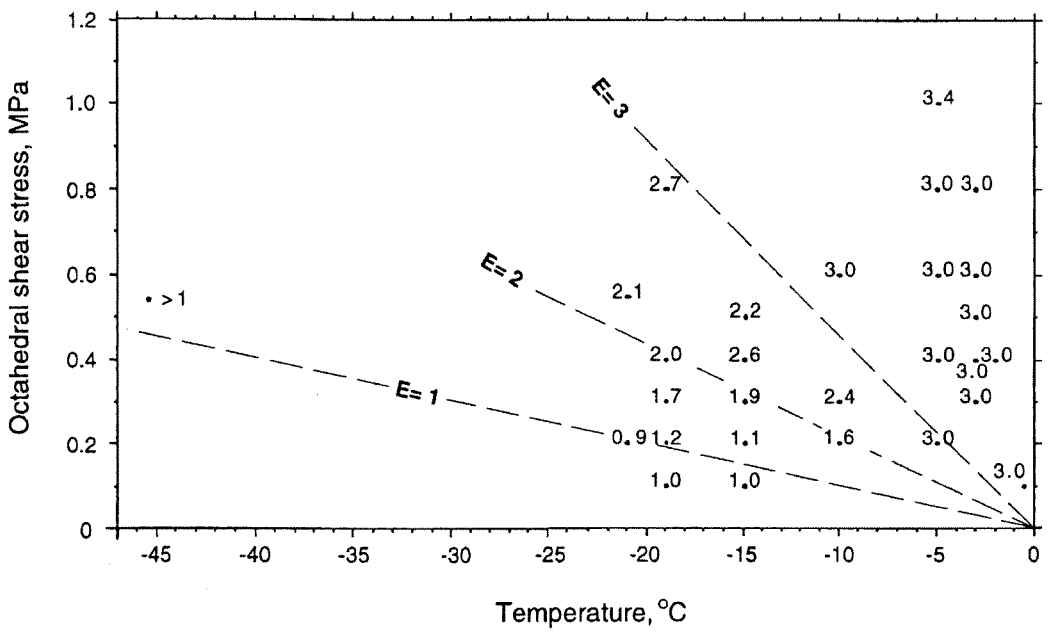

Figure 12: Map of enhancement factor, E plotted as a function of octahedral shear stress and temperature. Dashed lines are contours of E = 1, 2 and 3. The E = 1 line has been extended to –45 °C, where the 0.55 MPa test shows E values >1. Additional E = 3.0 data have been added from previous studies [1, 2].

that migration recrystallization is the dominant mechanism controlling flow rate at higher temperatures and stresses, but that it degenerates as temperature and stress are reduced, to the point where it has an insignificant influence on the flow.

Finally, in Fig. 12 we present from the data, a map of enhancement factor, E as a function of temperature and stress. We do this by contouring values of E over the stress/temperature domain, and it appears that (within the temperature and stress range studied) straight lines are sufficient to "define" the E field. We propose for flow interpretation from ice core fabric studies, and for polar ice sheet modelling studies, that this E field might be used to refine calculations of flow rates as a function of temperature and stress in regions of ice sheet compression.

References

1. W.F. Budd and T.H. Jacka, *Cold Reg. Sci. Technol.*, 16(2), 107-144 (1989).
2. T.H. Jacka and M. Maccagnan, *Cold Reg. Sci. Technol.*, 8(3), 269-286 (1984).
3. A.J. Gow, *IASH Publ.* 61, 272-284 (1963).
4. W.F. Budd, *Zeitschr. Gletscherkunde Glazialgeologie*, VIII, (1-2), 65-105 (1972).
5. A.J. Gow and T. Williamson, *CRREL Report* 76-35, 25 pp. (1976).
6. S. Herron, Physical properties of the deep ice core from Camp Century, Greenland. *Ph.D. Thesis, University of New York at Buffalo*, 146 pp. (1982).
7. S. Herron, C.C. Langway, Jr. and K.A. Brugger, *Geophys. Monograph* 33, AGU. 23-31 (1985).
8. Gao X.Q. and T.H. Jacka, In: Guo Kun (Ed.) *Proc. Internat. Symp. Antarctic Res.*, China Ocean Press, 41-52 (1989).
9. Li Jun, *Interrelation between flow properties and crystal structure of snow and ice. Ph.D. Thesis, The University of Melbourne*, 241 pp. (1995).
10. R.J. Thwaites, C.J.L. Wilson and A.P. McCray, *J. Glaciol.* 30(105), 171-179 (1984).
11. T. Thorsteinsson, J. Kipfstuhl and H. Miller, *J. Geophys. Res.* 102 (C12), 26,583-26,599 (1997).
12. A.J. Gow, D.A. Meese, R.B. Alley, J.J. Fitzpatrick, S. Anandakrishnan, G.A. Woods and B.C. Elder, *J. Geophys. Res.* 102(C12), 26,559-26,575 (1997).
13. V.I. Morgan, *Cold Reg. Sci. Technol.*, 19(3), 295-300 (1991).
14. Li Jun and T.H. Jacka, *Ann. Glaciol.* 29 (in press).
15. R.B. Alley, *Science*, 240(4851), 493-495 (1988).
16. R.B. Alley, *J. Glaciol.*, 38(129), 245-256 (1992).
17. N. Azuma and A. Higashi, *Ann. Glaciol.*, 6, 130-134 (1985).
18. N. Azuma and K. Goto-Azuma, *Ann. Glaciol.*, 23, 202-208 (1996).
19. O. Castelnau and P. Duval, *Ann. Glaciol.*, 20, 277-282 (1994).
20. T.H. Jacka and W.F. Budd, In: S.J. Jones, R.F. McKenna, J. Tollitson and I.J. Jordaan (Eds.), *Ice-Structure Interaction*, Springer-Verlag. 21-35 (1991).
21. J.W. Glen, *Proc. Roy. Soc., Series A.*, 228 (1175), 519-538.
22. Li Jun, T.H. Jacka and W.F. Budd, *Ann. Glaciol.*, 23, 247-252 (1996).
23. T.H. Jacka and R.C. Lile, *Cold Reg. Sci. Technol.*, 8(3), 235-240 (1984).

24. V.I. Morgan, *J. Glaciol.*, 22(87), 389-391 (1979).